THE JOURNAL OF BIOLOGICAL CHEMISTRY VOL. 284, NO. 32, pp. 21288–21295, August 7, 2009

Heteromeric *At*KC1·AKT1 Channels in *Arabidopsis* Roots Facilitate Growth under K^+-limiting Conditions*

Received for publication, May 8, 2009 Published, JBC Papers in Press, June 9, 2009, DOI 10.1074/jbc.M109.017574

Dietmar Geiger[‡], Dirk Becker[‡1], Daniel Vosloh[‡], Franco Gambale[§], Klaus Palme[¶], Marion Rehers[‖], Uta Anschuetz[‡], Ingo Dreyer[**], Jörg Kudla[‖], and Rainer Hedrich[‡]

From the [‡]Julius-von-Sachs-Institute, Molecular Plant Physiology and Biophysics, University of Wuerzburg, Julius-von-Sachs-Platz 2, D-97082 Wuerzburg, Germany, the [§]Istituto di Biofisica, Consiglio Nazionale delle Ricerche, Via de Marini 6, I 16149 Genova, Italy, the [¶]Department of Botany and Plant Physiology, Faculty of Biology, Albert-Ludwigs-University, Schaenzlestrasse 1, D-79104 Freiburg i. Br., Germany, the [‖]Institute for Botany and Botanical Garden, Molecular Developmental Plant Biology, University Muenster, Schlossplatz 4, 48149 Muenster, Germany, and the [**]Heisenberg Group of Biophysics and Molecular Plant Biology, Institute for Biochemistry and Biology, Karl-Liebknecht-Strasse 24/25, Haus 20, D-14476 Potsdam-Golm, Germany

Plant growth and development is driven by osmotic processes. Potassium represents the major osmotically active cation in plants cells. The uptake of this inorganic osmolyte from the soil in *Arabidopsis* involves a root K^+ uptake module consisting of the two K^+ channel α-subunits, AKT1 and *At*KC1. AKT1-mediated potassium absorption from K^+-depleted soil was shown to depend on the calcium-sensing proteins CBL1/9 and their interacting kinase CIPK23. Here we show that upon activation by the CBL·CIPK complex in low external potassium homomeric AKT1 channels open at voltages positive of E_K, a condition resulting in cellular K^+ leakage. Although at submillimolar external potassium an intrinsic K^+ sensor reduces AKT1 channel cord conductance, loss of cytosolic potassium is not completely abolished under these conditions. Depending on channel activity and the actual potassium gradients, this channel-mediated K^+ loss results in impaired plant growth in the *atkc1* mutant. Incorporation of the *At*KC1 subunit into the channel complex, however, modulates the properties of the K^+ uptake module to prevent K^+ loss. Upon assembly of AKT1 and *At*KC1, the activation threshold of the root inward rectifier voltage gate is shifted negative by approximately −70 mV. Additionally, the channel conductance gains a hypersensitive K^+ dependence. Together, these two processes appear to represent a safety strategy preventing K^+ loss through the uptake channels under physiological conditions. Similar growth retardation phenotypes of *akt1* and *atkc1* loss-of-function mutants in response to limiting K^+ supply further support such functional interdependence of AKT1 and AtKC1. Taken together, these findings suggest an essential role of *At*KC1-like subunits for root K^+ uptake and K^+ homeostasis when plants experience conditions of K^+ limitation.

Fundamental plant functions such as control of the membrane potential, osmo-regulation, and turgor-driven growth and movements are based on the availability to gain high cellular potassium concentrations (1). The absorption of this inorganic osmolyte from the soil by the root therefore represents a pivotal process for plant life. Classical experiments by Epstein *et al.* in 1963 (2) described K^+ root uptake as a biphasic process mediated by two uptake mechanisms: high affinity potassium transport with apparent affinities of ~20 μM and a low affinity transport system with K_m values in the millimolar range. During the last decades several molecular components of potassium transport systems have been identified and functionally characterized in plants (3, 4). Mutant analyses, heterologous expression, as well as radiotracer uptake experiments characterized the K^+ channels AKT1·*At*KC1 and members of the HAK·KT·KUP family as major components of the *Arabidopsis thaliana* root-localized potassium transport system (5–9). In this study we focused on AKT1 and *At*KC1, members of the *Arabidopsis* Shaker-like K^+ channel family. AKT1 is a voltage-dependent inward-rectifying K^+ channel mediating potassium uptake over a wide range of external potassium concentrations (10–15). Root cells of the *akt1-1* loss-of-function mutant completely lack inward rectifying K^+ currents (12). As a consequence the growth of *akt1-1* seedlings is strongly impaired on low potassium medium (100 μM and less) (11, 12, 15). Rescue of yeast growth on 20 μM K^+ and patch clamp experiments (16, 17) directly demonstrated that plant inward rectifying K^+ channels are capable of serving as high affinity potassium uptake transporters. *At*KC1 shares its expression pattern with AKT1 (18–20). *At*KC1 α-subunits, however, neither form functional channels in *akt1-1* knock-out plants nor in heterologous expression systems. In contrast to root cells of *akt1-1* loss of function mutants, root protoplasts of *At*KC1 null mutants (*atkc1-f*) still exhibit inward rectifying potassium currents most likely derived from homomeric AKT1 tetramers (20). Inward K^+ currents in this *atkc1-f* mutant were characterized by a more positive activation voltage. These data suggested that the *At*KC1 α-subunits do not form K^+ channels *per se* but modulate the properties of the AKT1·*At*KC1 heterocomplex (20–22). Previously, two groups in their groundbreaking studies demonstrated that AKT1 is activated by the CBL[2]-interacting, serine/threonine kinase, CIPK23, particularly under low K^+ conditions (23, 24). CIPK23 itself was shown to be activated by the two calcineurin B-like proteins, CBL1 and 9, act-

* This work was supported by a Heisenberg Fellowship from the Deutsche Forschungsgemeinschaft (to I. D.) and by Deutsche Forschungsgemeinschaft Research Group Grant FOR964 (to R. H., J. K., and D. B.).

[1] To whom correspondence should be addressed. Tel.: 49-931-888-6108; Fax: 49-931-888-6157; E-mail: dbecker@botanik.uni-wuerzburg.de.

[2] The abbreviations used are: CBL, calcineurin-B-like protein; CIPK, CBL-interacting protein kinase; WT, wild type; BiFC, bimolecular fluorescence complementation; MES, 4-morpholineethanesulfonic acid; YFP, yellow fluorescent protein.

ing in a Ca^{2+}-dependent manner upstream of CIPK23 (25, 26). Genetic disruption of these elements resulted in transgenic plants exhibiting a phenotype comparable with that of the AKT1 loss of function mutant. This regulatory system, based on a calcium sensor, a protein kinase, and a K^+ channel, was functionally reconstituted in *Xenopus* oocytes (23, 24, 27), suggesting that these elements are essential and sufficient to operate as a low K^+-sensitive potassium uptake system. Here we report on the physiological properties of the heteromeric K^+ uptake module formed by the predominant root potassium uptake channel subunits, AKT1 and *At*KC1 and its regulating kinase complex, CBL1 and CIPK23. Our studies show that the physical interaction of the CBL1·CIPK23 complex is specific for AKT1 channels and does not involve the *At*KC1 subunit. AKT1 possesses a K^+ (absence) sensor affecting channel activity at submillimolar K^+ concentrations by strongly reducing its maximal cord conductance. Despite this K^+ sensor, upon activation, AKT1 homomeric channels were shown to represent a potassium leak at low external potassium concentrations. Integration of *At*KC1 into the K^+ uptake module, however, prevented potassium loss by modulating both the voltage sensor and conductance in the channel complex. Moreover, activation of the AKT1-like maize channel ZMK1 by CBL1·CIPK23 suggests a conserved interaction and regulation across monocot and dicotyledonous plant species. Our biophysical studies as well as growth assays with plant mutant lines lacking the respective channels underline that acquisition of potassium under limiting K^+ conditions is mediated via the root AKT1·*At*KC1 K^+ uptake channel complex.

MATERIALS AND METHODS

Growth Assay—The dependence of seedling growth on extracellular K^+ was measured on sterile agarose medium containing a defined ionic composition as previously described (12). Growth of *akt1-1* mutant was compared with Wassilevskija WT seedlings and *atkc1-f* mutant to Col-0 WT seedlings. The fresh weight as well as the root length of WT and mutant seedlings was determined after 11 days of seedling growth under a 12/12-h light to dark rhythm. 2 mM NH_4^+ was added to the medium to inhibit transporter-mediated K^+ uptake (11, 12, 15). Root length and the fresh weight of at least 20 seedlings were measured at each condition in three independent experiments (±S.D.).

Molecular Biology—To generate cRNAs for CBLs and CIPKs, full-length cDNAs for CBL1, 4, 5, and 9 and CIPK1, 11, 12, 16, 17, 19, 22, 23, and 24 were cloned in oocyte expression vectors and verified by sequencing. For oocyte BiFC experiments these cDNAs were fused to the N- or C-terminal half of an YFP cDNA. For functional analyses cRNA of AKT1, *At*KC1, ZMK1, KAT1, and the members of the CBL and CIPK kinase families was prepared using the mMessage mMachine T7 transcription kit (Ambion, Austin, TX). Oocyte preparation and cRNA injection have been described elsewhere (28). AKT1, *At*KC1, and ZMK1 cRNA (10–20 ng) was injected in combination with 0.5 ng of cRNA of CBL1 and CIPK23, respectively, unless stated otherwise.

Yeast Two-hybrid and BiFC Studies—Yeast transformation and two-hybrid analyses were performed as described (29, 30) with the exception that the yeast strain PJ69-4A (31) was used, and the yeast were incubated at 23 °C on medium supplemented with 2.5 mM 3-amino-1,2,4-triazole. The generation of the CBL and CIPK two-hybrid constructs has been described (30). To generate the additional constructs used in this study, the C-terminal regions of *At*KC1 (amino acids 330–662) and AKT1 (from amino acid 220) were amplified by PCR and after sequence verification were cloned into pAD-GH as described (30). For *in planta* BiFC studies, the full-length AKT1 cDNA construct was amplified by PCR and cloned with XbaI-XmaI into pSPYCE-35S, whereas *At*KC1 cDNA was cloned with BamHI-XhoI into pSPYNE-35S. Infiltration of *Nicotiana benthamiana* leaves was performed as described (30). Protoplasts were prepared 3 days after infiltration by incubating leaf discs in 500 mM mannitol, 10 mM $CaCl_2$, 5 mM MES/KOH, pH 5.5, 3% cellulase, and 0.75% Macerozym. For documentation of the results, pictures were taken on an inverted microscope (Leica DMIRE2) equipped with the Leica TCS SP2 laser-scanning device.

Electrophysiology—In two-electrode voltage-clamp studies, oocytes were perfused with KCl-containing solutions, based on Tris/MES buffers. The standard solution contained 10 mM MES/Tris, pH 5.6, 1 mM $CaCl_2$, 1 mM $MgCl_2$, and 30 mM KCl. Osmolarity was adjusted to 220 mOsmol/kg using D-sorbitol. The ionic strength was adjusted with LiCl to 100 mM. To inhibit oocyte endogenous currents, especially at potentials negative from −160 mV, 1 mM $LaCl_3$ was added to the bath solution (32). It was verified that $LaCl_3$ had no effect on the K^+ channel activity. Voltage-dependent activation of KAT1, AKT1, and AKT1·*At*KC1 heterotetramers was recorded using single-pulse protocols. Starting from a holding potential (V_H) of −20 mV, a series of voltage pulses were applied as indicated in the figure legends. Steady state currents, I_{SS}, measured at the end of the activation pulses (voltage, V) were well described by the equation,

$$I_{SS} = G_{K_{max}} \times (V - V_{rev})/(1 + \exp(zF(V - V_{1/2})/RT)) \quad \text{(Eq. 1)}$$

where V_{rev} is the reversal voltage, *i.e.* the voltage at which the electrical gradient compensates the chemical K^+ gradient; $V_{½}$ is the half-maximal activation potential; z is the apparent gating charge; and $G_{K\text{-}max}$ is the maximal conductance. Subsequently, channel cord conductance was extracted according to the following equation.

$$G_K = I_{SS}/(V - V_{rev}) \quad \text{(Eq. 2)}$$

This calculation eliminates the chemical driving force of the K^+ gradient.

RESULTS

Growth Retardation in akt1-1 and atkc1-f Mutants under K^+ Starvation—The voltage-dependent potassium channel AKT1 is activated during K^+ starvation in a calcium- and phosphorylation-dependent manner (23). In addition to AKT1, root cells express the structural homologues *At*KC1 and GORK (18, 20). In contrast to AKT1 and *At*KC1, the GORK protein represents a K^+ outward rectifier (efflux) channel. To investigate the contribution of *At*KC1 to channel-mediated high affinity K^+

uptake in roots, we compared K^+-dependent seedling growth of the *A. thaliana* mutants *akt1-1* and *atkc1-f* with that of the respective wild types (Wassilevskija, Col-0; Fig. 1). On medium containing as low as 100 μM K^+, *akt1-1* seedlings appeared significantly impaired in root growth (57% +/− 4.5%). Lowering the K^+ concentration to 10 μM, WT as well as *akt1-1* seeds failed to fully emerge from the seed coat (11, 12). At 100 μM K^+ the root length of the *atkc1-f* mutant was reduced by ~28% (+/− 6.0%) and was less affected than the *akt1-1* seedlings. This observation is in line with the fact that root cells of the *atkc1-f* mutant still conduct inward potassium currents, most probably carried by AKT1 homomers (20). At 10 μM K^+, seedling emergence from the seed coat in *atkc1-f* was as drastically impaired as in *akt1-1* and the corresponding WT seedlings. Similar data were obtained for differences in fresh weight (data not shown).

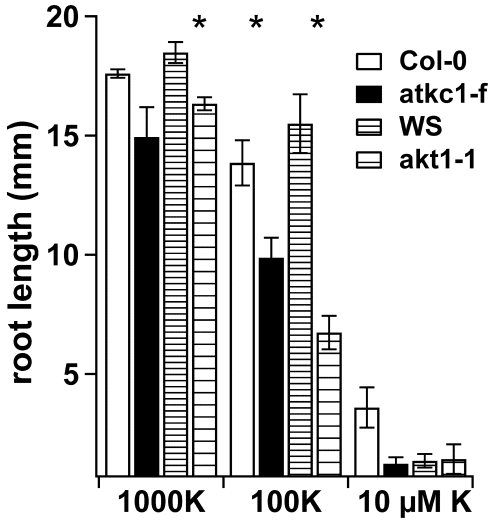

FIGURE 1. ***A. thaliana* seedling growth under limiting K^+ conditions.** K^+ concentrations are given in μM. The root length of at least 20 seedlings was measured at each condition in three independent experiments (±S.D.). The *asterisks* indicate statistically significant differences compared with WT (calculated by a two-tailed Student's *t* test, $p < 0.05$).

Notably, Col-0 WT seeds performed better under potassium-limiting conditions than Wassilevskija-0 seeds. These results indicate that under potassium starvation, both K^+ channel α-subunits contribute to the K^+ uptake system of *Arabidopsis* roots.

CIPK23-specific Activation of AKT1—Studies by Xu *et al.* (23) and Li *et al.* (24) provided first evidence for a phosphorylation-dependent activation of the AKT1 channel during K^+ starvation. As shown for the *akt1-1* and the *atkc1-f* mutant, transgenic plants lacking either the serine/threonine protein kinase CIPK23 or the two Calcineurin B-like proteins CBL1 and CBL9 exhibited impaired growth on low potassium concentrations (23, 24). To study the properties of the K^+ uptake channel complex in detail, we performed voltage clamp measurements with oocytes co-expressing AKT1 and a CBL·CIPK pool containing the plasma membrane-localized CBLs 1, 4, 5, and 9 and root-expressed CIPKs 1, 11, 12, 16, 17, 19, and 22 except CIPK23 (Fig. 2*A*, *upper traces*). This pool of kinases failed to evoke AKT1-mediated macroscopic potassium currents. The addition of CIPK23 cRNA to the CBL·CIPK mix, however, resulted in typical AKT1 hyperpolarization-activated inward rectifying K^+ currents (Fig. 2*A*, *lower traces*). This finding points to a highly specific protein-protein interaction between AKT1 and CIPK23. When the AKT1 orthologue from maize, ZMK1, was co-expressed with the identical pools of kinases, similar inward rectifying K^+ channel activation was monitored only in the presence of CIPK23 (Fig. 2*B*). This observation indicated that a CBL·CIPK-mediated channel activation mechanism is conserved among different plant species. *At*KC1 co-expressed with the CBL·CIPK pool, however, remained electrically silent (data not shown), pointing to a specific interaction between CIPK23 and AKT1.

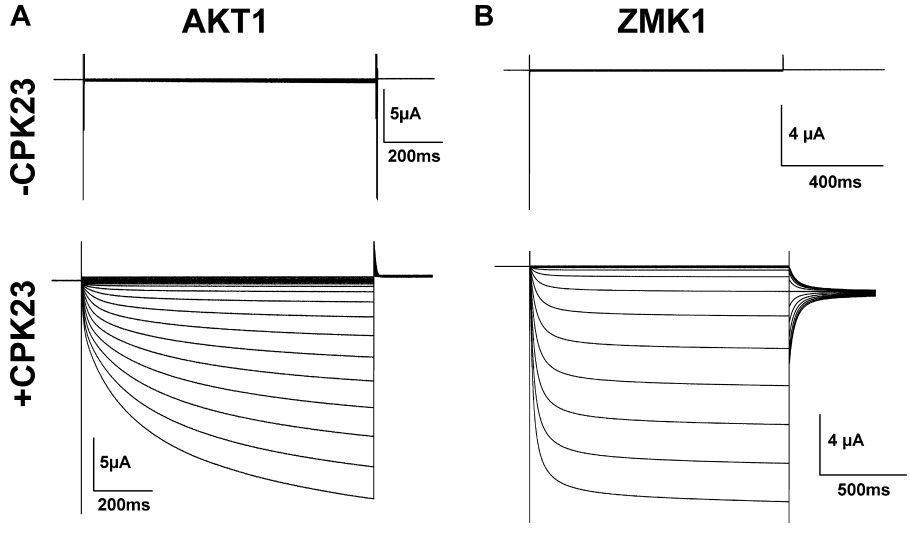

FIGURE 2. **Specificity of AKT1/CIPK23 and ZMK1/CIPK23 interaction.** Whole oocyte voltage-clamp measurements at membrane potentials ranging from 20 to −160 mV in 10-mV decrements in the presence of 100 mM KCl are shown. *A*, K^+ currents of an oocyte co-injected with AKT1 and a CBL·CIPK pool containing CBL 1, 2, 4, 5, and 9 and CIPK 1, 11, 12, 16, 17, 19, and 22 (*upper traces*) and current response of a representative oocyte injected with AKT1 cRNA together with the given CBL·CIPK pool complemented with CIPK23 cRNA (*lower traces*). *B*, identical experiments were performed with ZMK1 instead of AKT1. Like the activation of AKT1 in *A*, ZMK1 was specifically activated by CIPK23.

We used the yeast two-hybrid system to test the direct interaction of AKT1 and *At*KC1 with CIPKs. To this end, the C-terminal cytosolic regions of AKT1 (starting from amino acid His^{294}) and *At*KC1 (starting from amino acid His^{330}) were cloned in activation domain vectors, and interaction with full-length CIPKs in binding domain vectors was analyzed by growth on selective media. As depicted in Fig. 3*A*, this analysis revealed interaction of AKT1 with CIPK23 as indicated by growth on selective media. Combination of AKT1 with CIPK1 did not rescue growth in these assays, indicating the specificity of the observed interaction with CIPK23. In contrast to AKT1, combination of *At*KC1 with either CIPK23 (Fig. 3*A*) or any other of the 25 CIPKs (data not shown) did

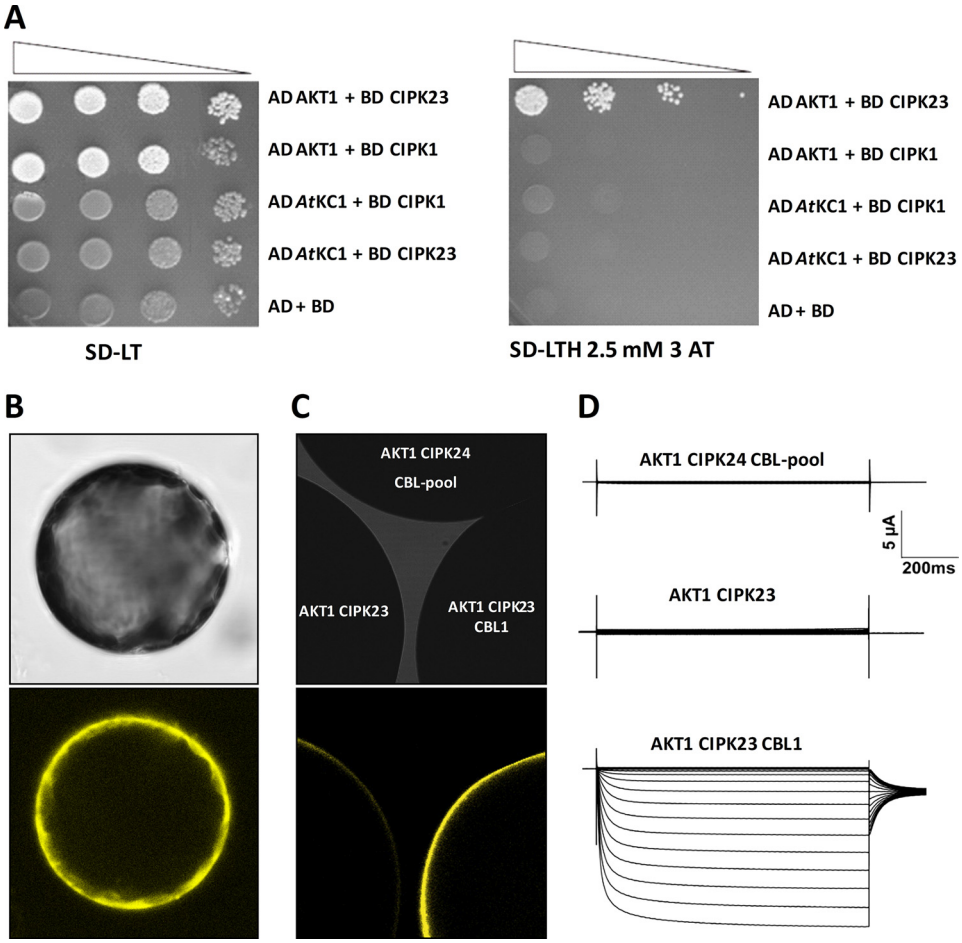

FIGURE 3. **AKT1·CIPK23 interaction and *At*KC1·AKT1 heterotetramerization.** *A*, interaction studies of AKT1 and *At*KC1 with CIPKs in yeast. The yeast strain PJ69-4A containing the indicated plasmid combinations was grown on SD medium -LT to an *A*600 of 2. Ten microliters of 10-fold dilution series were spotted onto selective (SD-LTH 2.5 mM 3-amino-1,2,4-triazole) and nonselective (SD-LT) media. Decreasing cell densities in the dilution series are illustrated by *narrowing triangles*. The photographs were taken after 14 days growth at 23 °C. *B*, heterotetramerization of *At*KC1 with AKT1; *At*KC1/AKT1 interaction in plant cells studied by bimolecular fluorescence complementation (30). Faithful expression of all YFP fusion proteins in these assays was confirmed by Western blot analyses using monoclonal antibodies against the fusion tags (data not shown). *C* and *D*, AKT1/CIPK interaction studies in representative *Xenopus* oocytes by BiFC (*C*) and subsequent two-electrode voltage clamp recordings of the same oocyte (*D*). Only the co-expression of AKT1 together with CIPK23 and CBL1 complemented YFP fluorescence and resulted in macroscopic K^+ currents. CIPK24 and a pool of CBLs (1, 4, 5, and 9) or CIPK23 alone co-expressed with AKT1 resulted neither in specific BiFC signals nor in K^+ currents.

not restore growth. To reassess the yeast two-hybrid data, we employed BiFC to follow physical interactions of channels and kinases in *Xenopus* oocytes. For this purpose we fused the C-terminal half of a YFP to the C terminus of AKT1 (AKT1::YFP CT) and the N-terminal half of an YFP to the C terminus of CIPK23 (CIPK23::YFP NT). Expression of any of these constructs alone did not result in YFP fluorescence (data not shown). Co-expression of AKT1::YFP CT and CIPK23::YFP NT did not lead to macroscopic AKT1 currents in oocytes (Fig. 3*D*, *middle panel*), and in plant cells fluorescence complementation caused by AKT1::YFP CT CIPK23::YFP NT interaction was rather weak. Expressing these constructs together with CBL1, however, resulted in typical AKT1 K^+ currents (Fig. 3*D*, *bottom panel*) and bright YFP fluorescence monitored by confocal microscopy (Fig. 3*C*). This indicates that physical interaction between AKT1 and CIPK23 occurs mainly in the presence of CBL1, which seemed to act as a scaffold protein. As a control AKT1::YFP CT was expressed together with CIPK24::YFP NT and a pool of CBLs (1, 4, 5 and 9). This combination did not show fluorescence complementation. In line with this result, the co-expression of AKT1 with the CIPK24/CBL pool did not result in detectable K^+ currents in oocytes (Fig. 3, *C* and *D*, *top panels*). Like their animal counterparts, functional plant *shaker*-like K^+ channel proteins are formed by four α-subunits (33–35). Furthermore it was suggested that the heteromeric assembly of different α-subunits might provide for the molecular basis of the broad functional diversity observed *in planta* (34, 36, 37). To directly investigate the potential physical interaction of AKT1 with *At*KC1 in plant cells, we again used the BiFC technique in *N. benthamiana* protoplasts. In these assays, formation of heteromeric AKT1·*At*KC1 complexes was observed at the plasma membrane (Fig. 3*B*). Importantly, no fluorescence was observed in control transformations expressing either AKT1 or *At*KC1 in combination with the complementary half of YFP (data not shown). Taken together, our data provide strong evidence for the formation of AKT1·*At*KC1 heterotetramers in plant cells. They further suggest that, although both AKT1 and *At*KC1 contribute to the K^+ uptake system in *Arabidopsis* roots, only the AKT1 subunit represents a target for phosphorylation by calcium-dependent CBL·CIPK complexes.

AKT1 Homomers Represent Potassium Leaks—To study AKT1-mediated high affinity K^+ uptake following activation by CBL·CIPK, we monitored channel activity at external potassium concentrations mimicking K^+-depleted soils. Fig. 4 (*A* and *B*) shows that in medium containing 0.5–1 mM K^+, pronounced outward currents were recorded in a voltage window between −40 mV and the reversal potential for K^+ (E_K) at which currents reversed their direction. Thus, under these conditions, AKT1-expressing cells leaked potassium ions (Fig. 4*B*). Peak K^+ efflux was higher at 0.5–1 mM compared with 100 or 10 μM external K^+, despite the increased driving force for K^+ release at lower external potassium. It became apparent that inward currents, negative of E_K, almost disappeared at limiting K^+ concentrations (100–10 μM) and pointed to gating control of AKT1 by extracellular potassium ions. A Boltzmann analysis of voltage-dependent channel activity revealed a consistent half-maximal activation potential ($V_{½}$)

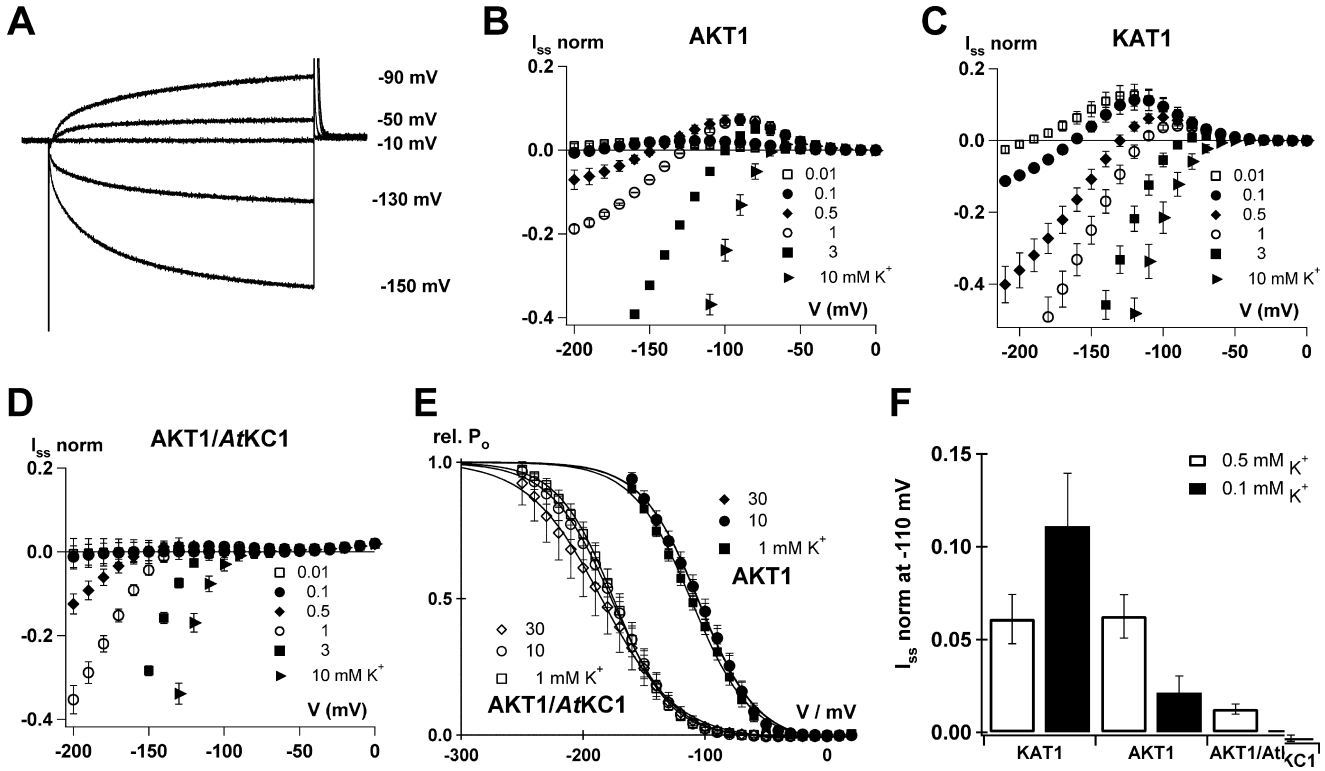

FIGURE 4. **Biophysical analysis of channel-mediated K^+ currents at limiting extracellular K^+ concentrations.** *A*, current response of an AKT1, CBL1 CIPK23 co-injected oocyte to given membrane potentials in 1 mM K^+. Macroscopic outward currents appeared at membrane potentials positive from E_K. *B*, steady state currents (I_{SS}) of AKT1 injected oocytes at K^+ concentrations ranging from 0.01 to 10 mM plotted against the membrane potential. Note that positive from E_K potassium is released, whereas negative from E_K K^+ is taken up. Although the driving force for K^+ release is maximized with ongoing K^+ depletion, outward currents decreased when K^+ concentrations were <0.5 mM. The currents were normalized to the value gained at −150 mV in 10 mM KCl ($n = 4 \pm$ S.D.). *C*, *I/V* plot of KAT1 expressing oocytes monitored under the same conditions as in *B*. In contrast to AKT1, K^+ release mediated by KAT1 appeared even more pronounced upon lowering external K^+ ($n = 3 \pm$ S.D.). *D*, steady state currents of AKT1·*At*KC1 co-injected oocytes were plotted against the membrane voltage. In contrast to KAT1 and AKT1 homomers, heterotetrameric AKT1·*At*KC1 channels did not allow significant K^+ release at extracellular K^+ concentrations as low as 0.01 mM ($n = 4 \pm$ S.D.). *E*, the relative open probability (*rel.* P_o) of AKT1 (*filled symbols*) and AKT1·*At*KC1 complexes (*open symbols*) expressed in oocytes at external K^+ concentrations of 1, 10, and 30 mM plotted against the test voltage. Note the prominent negative shift of the half-maximal activation potential ($V_{1/2}$) because of the integration of *At*KC1 subunits into the channel complex. The data points were fitted with a Boltzmann function (*line*; $n = 5 \pm$ S.D.). *F*, comparison of steady state currents of KAT1, AKT1, and AKT1·*At*KC1 injected oocytes measured at −110 mV in 0.5 and 0.1 mM extracellular potassium. Note that in contrast to KAT1 outward currents of the AKT1 homomer and the AKT1·*At*KC1 heteromer decreased upon lowering the K^+ concentration from 0.5 to 0.1 mM.

of −107 mV (± 3.4 mV) and a slope factor (corresponding to a gating charge) of 1.0 (± 0.05) for AKT1 homomers in the K^+ concentration range between 1 and 30 mM (Fig. 4*E*). This shows that at high extracellular potassium concentrations, AKT1 gating is independent of K^+, a feature previously described for voltage-dependent guard cell K^+ channels such as KAT1 and KAT2 (17, 38). Indeed, alike AKT1, KAT1 exhibited pronounced K^+ leakage at limiting external K^+, too (Fig. 4*C*). Thus, in the voltage range between E_K and the threshold voltage for channel activation, AKT1 homomers cannot avoid K^+ efflux at low K^+ concentrations (Fig. 4*B*). Because of these gating characteristics, K^+-limiting conditions could open up a shunt pathway for K^+ in AKT1-expressing root cells (*cf.* Fig. 1).

AtKC1 Prevents AKT1-mediated Potassium Loss—In the absence of *At*KC1, K^+ currents in Arabidopsis root cells activate 50 mV more positive compared with WT protoplasts expressing both *At*KC1 and AKT1 (20). In experiments with AKT1 homomeric channels expressed in *Xenopus* oocytes, we reconstructed the behavior of the *atkc1-f* mutant (Fig. 4, *A* and *B*). To mimic the situation of *Arabidopsis* WT root cells in *Xenopus* oocytes, we co-injected AKT1·CBL1·CIPK23 and the *Shaker* channel α-subunit *At*KC1. As a result $V_{½}$ of the inward rectifying potassium currents was −179 ± 5.5 mV and thus shifted by more than −70 mV when compared with AKT1 homomers (Fig. 4*E*). This behavior confirms the notion that both K^+ channel α-subunits assemble into a channel holoprotein that forms the root K^+ uptake complex *in planta*. In addition, in the presence of *At*KC1, a strong reduction of potassium leakage was observed at limiting external K^+ (Fig. 4*D*). To elaborate this effect further, we compared the steady currents at −110 mV mediated by KAT1, AKT1, and AKT1·*At*KC1 (Fig. 4*F*). In KAT1 the outward K^+ currents increased with increasing driving force (0.5–0.1 mM K^+_{ext}). In contrast, AKT1 homomeric channels exhibited decreasing potassium loss when lowering the external potassium concentration below 0.5 mM, whereas in AKT1·*At*KC1 heteromeric channel outward K^+ currents tended to zero over a wide range of external K^+ concentrations. Taken together, these results suggest that AKT1 alone as well as AKT1·*At*KC1 heteromers exhibit an intrinsic K^+ sensor highly sensitive to decreasing external potassium availability.

Decreasing Extracellular Potassium Inactivates the Root K^+ Uptake Channel Complex—To gain further insights into the molecular basis of channel activity at different external K^+ concentrations, we performed a quantitative comparison of activa-

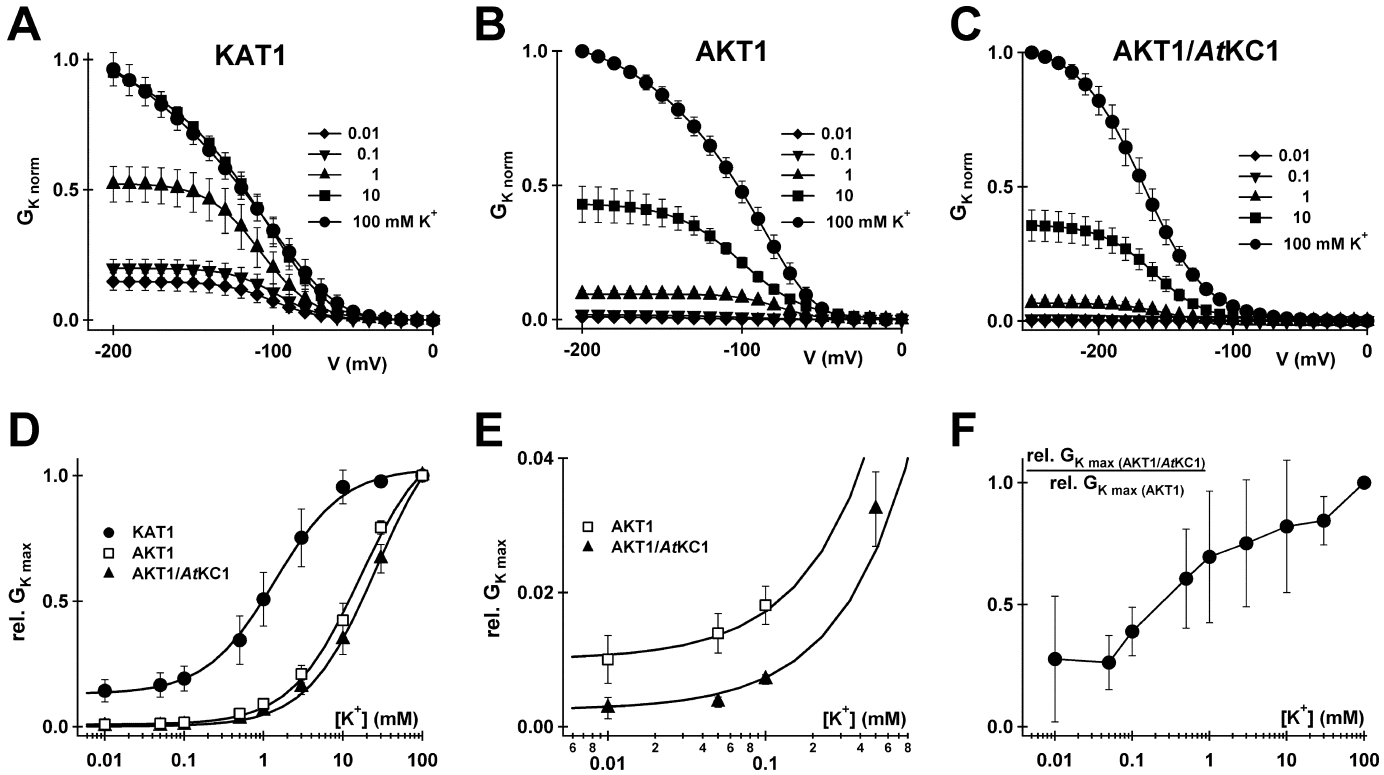

FIGURE 5. **Removal of external K^+ decreases AKT1 and AKT1·*At*KC1 cord conductance.** *A–C*, G_K/V relation of KAT1-, AKT1-, and AKT1·*At*KC1-expressing oocytes evaluated at the indicated K^+ concentrations. The data points were normalized to 1 at the cord conductance in 100 mM potassium at −200 mV (AKT1 and KAT1) or at −250 mV (AKT1·*At*KC1) and fitted with a Boltzmann function (*solid lines*). Note that the reduction of external K^+ resulted in a decrease of conductance ($n \geq 3 \pm$ S.D.). *D*, the relative cord conductance (*rel.* $G_{K\text{-}max}$) was calculated as relative $G_{K\text{-}max} = G_{K\text{-}max}(\times \text{mM})/G_{K\text{-}max}(100\ \text{mM})$ and plotted against the K^+ concentration in a semi-logarithmic plot. The data points were fitted by a Hill function (Equation 3, *solid lines*). Note that $G_{K\text{-}max}$ of AKT1 and AKT1·*At*KC1 decreased steeply already at moderate K^+ concentrations of ~10–30 mM. Under these conditions the conductance of KAT1 remained on a high level. *E*, magnification of relative $G_{K\text{-}max}$ of AKT1 and AKT1·*At*KC1 at low external K^+ concentrations. The formation of AKT1·*At*KC1 heteromeric channels reduced the cord conductance under limiting K^+ conditions by more than 50% compared with the AKT1 homomer. *F*, ratio of the relative cord conductances of AKT1·*At*KC1 and AKT1. Values <1 indicate a smaller cord conductance of AKT1·*At*KC1 compared with that of AKT1.

tion curves by analyzing the channel cord conductance. This procedure eliminates the chemical driving force of the K^+ gradient and shows that the resulting G_K/V relations obtained at various K^+ concentrations were well described by Boltzmann functions (Fig. 5, *A–C*). The resulting plot consistently revealed that G_K for KAT1, AKT1, as well as for AKT1·*At*KC1 decreased upon lowering the external K^+ concentration from 100 mM down to 10 μM. However, whereas KAT1 channel activity was similar in high external K^+ (100 and 10 mM; Fig. 5*A*), decreasing the external potassium concentration from 100 to 10 mM resulted in a drastic reduction of ~55 and 63% in AKT1 and AKT1·*At*KC1, respectively (Fig. 5, *B* and *C*). For the latter, this effect was even more pronounced at K^+ concentrations below 10 mM. How can this behavior be explained? First, a reduction of the AKT1 single channel conductance could have caused a reduction in G_K. Second, the observed gradual decrease in G_K was brought about by a reduction in the number of active channels. In this regard, Hertel *et al.* (39) reported that the *Arabidopsis* potassium channel KAT1 is K^+-sensitive in the micromolar range. Furthermore, it was shown that G_K was reduced upon depletion of external potassium because of the reduction of the number of active channels. When plotting the calculated maximal $G_{K\text{-}max}$ *versus* the external potassium concentration (Fig. 5*D*), data points could be well fitted with a Hill equation of the following form,

$$G_{K\text{-}max} = G_{min} + \frac{G_{max} - G_{min}}{1 + \left(\frac{K_{0.5}}{[K^+]}\right)^n} \qquad \text{(Eq. 3)}$$

where $K_{0.5}$ is the concentration for half-maximal inhibition, and n denotes the Hill factor. When fitted with integer numbers for n of 1–3, the best results were obtained with a Hill coefficient of 1 and a $K_{0.5}$ of 1.4 ± 0.1 for KAT1. For AKT1 this curve ($K_{0.5}$ = 16.2 ± 1.5 mM) shifted strongly toward higher potassium concentrations (Fig. 5*D*) indicative for an intrinsic sensor. As shown in Fig. 5 (*E* and *F*), the AKT1·*At*KC1 complex, however, was even more sensitive toward low K^+ than the AKT1 homomer. A $K_{0.5}$ of 26.0 ± 1.5 mM reflects a dramatically reduced channel conductance by 50–75% at low external K^+ concentrations (0.5 mM and less). Thus, besides the negative shift in the activation threshold, this root K^+ channel complex exhibits an enhanced sensitivity to low external K^+ as a second mechanism to avoid the loss of cytosolic K^+ toward potassium-depleted soils.

DISCUSSION

Seedlings lacking the modulatory K^+ channel α-subunit *At*KC1 (*atkc1-f*) are restricted in their growth on limiting K^+ concentrations similar to *akt1-1* knock-out plants. Previous studies have shown that the lack of *At*KC1 causes pronounced changes in the

biophysical properties of the AKT1-based root K^+ uptake channel complex (18, 20). We thus studied the physiological relevance of channel heteromer formation and the molecular mechanism providing for channel mediated regulation of K^+ homeostasis in root cells under conditions of limiting potassium supply. Electrophysiological studies enabled us to dissect the individual contribution of AKT1 and *At*KC1 to low K^+ uptake.

Assuming a cytosolic K^+ concentration of ~100 mM in root cells and soil potassium concentrations ranging from 100 to 10 μM, the reversal potential for K^+ (E_K) would range between −180 and −240 mV, respectively. Under this condition the root cell membrane potential has to be strongly and permanently hyperpolarized to allow channel-mediated K^+ uptake. Lack of any of the predominant root K^+ uptake channel, AKT1 or *At*KC1, resulted in impaired growth performance of the respective mutants under potassium-limiting conditions (Fig. 1 and Refs. 11, 12, 15, and 20). This finding is not surprising for the *akt1-1* mutant, which apparently lacks any K^+ uptake channel activity (20). The *atkc1-f* mutant, however, still exhibits AKT1-mediated K^+ currents as deduced from respective patch-clamp studies on root hair protoplasts. Thus, a pivotal role for *At*KC1 in potassium homeostasis may be proposed under conditions of low K^+ supply. Recently, activation of AKT1 was shown to require the cytosolic calcium sensors CBL1/9 and its interacting kinase CIPK23 (23, 24). In the absence of *At*KC1, however, CBL·CIPK-mediated phosphorylation of AKT1 is apparently not sufficient to allow plants to cope with K^+ starvation (Fig. 1). Furthermore, *At*KC1 does not appear to be a target of CIPK23, as deduced from our yeast two-hybrid and fluorescence-based interaction studies (Fig. 3). Consequently, the low K^+ phenotype of the *atkc1-f* mutant appears directly related to the biophysical properties of the remaining AKT1 channel. Our studies show that at low K^+ and in the absence of *At*KC1 root K^+ uptake channels open at voltages positive of E_K, a condition driving K^+ efflux through the open inward rectifier. This behavior is observed for AKT1 as well as for the guard cell K^+ uptake channel KAT1 (Fig. 4). In contrast to KAT1, however, which exhibits considerable channel activity down to micromolar K^+ concentrations, AKT1 appeared largely inactivated under those conditions (Figs. 4 and 5). Thus, one mechanism to prevent massive K^+ loss resides in the AKT1-intrinsic K^+ (absence) sensor. This atypical behavior is reminiscent to gating control by the selectivity filter (40). Biophysical and structural studies on animal and plant K^+ channels suggest that this K^+ sensor resides in the pore-forming loop including the outer pore vestibule of these ion channels (41–44). According to these models, lowering the extracellular K^+ concentration beyond a channel-specific threshold results in a conformational change/collapse of the structural integrity of the pore and in subsequent channel inactivation rather than changes in single channel conductance or mean open times. This hypothesis is further supported by the finding that permeable ions such as Rb^+ or Cs^+, blocking the open channel, but not the impermeable ions Li^+ or Na^+, were capable of mimicking the pore stabilizing effect of K^+ (41, 43). Although the overall pore geometry for *shaker*-like potassium channels is assumed to be very similar, the actual, critical K^+ concentration responsible for channel inactivation differs among members of this subfamily.

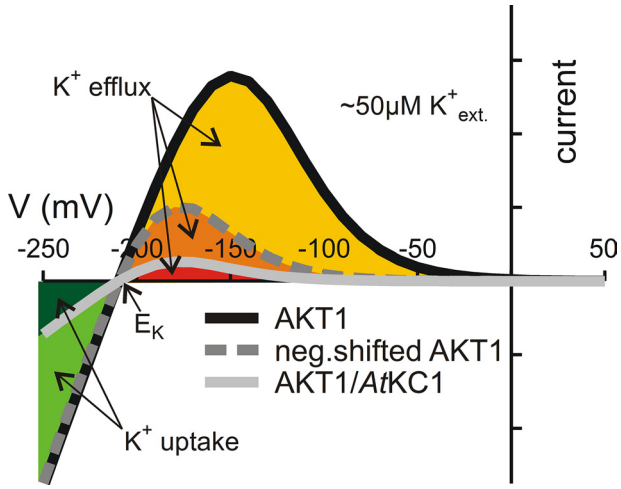

FIGURE 6. **AtKC1 modulates the activity of AKT1.** The effect of the involvement of *At*KC1 on the properties of the root inward rectifier under limiting external K^+ conditions (~50 μM). Under these conditions AKT1 homomeric channels would allow macroscopic K^+ release at voltages positive from E_K (*black curve*, *yellow area*). Integration of the *At*KC1 subunit into the root inward rectifier complex shifts the voltage-dependent gating of AKT1 to more negative membrane potentials (*dotted gray curve*). Thereby the K^+ release at depolarized membrane potentials would be reduced but not completely prevented (*orange area*). Besides, the shift in voltage-dependent gating, *At*KC1 further reduces the relative conductance (*solid gray curve*). The combination of these two effects inhibits massive K^+ loss (*red area*) and still allows K^+ uptake at membrane potentials negative from E_K (*dark green area*). AtKC1 therefore modulates the activity of the root K^+ inward rectifier and fine tunes its electrophysiological properties according to the availability of extracellular potassium.

Thus, although the potassium-sensing feature is shared among AKT1 and, for example, KAT1 (39), they exhibit a subtle but essential distinction in the affinity toward external K^+. Deduced from Hill plots of the potassium-dependent cord conductance, we calculated a single accessible binding site for potassium ions in the AKT1 channel with an apparent affinity constant of ~16.2 mM. This results in pronounced K^+ leakage already at moderate external K^+ supply and negatively feeds back on growth performance (Figs. 1 and 6). In comparison with the guard cell inward rectifier KAT1, we obtained a much lower constant of ~1.4 mM. Although this property ensures KAT1 channel activity over a wide range of external potassium concentrations (down to the micromolar range), it would favor K^+ loss with increasing driving forces (decreasing external K^+) and thus renders KAT1-like channels unsuitable for controlling root K^+ homeostasis.

The low K^+ affinity binding site of AKT1 lowers the maximal cord conductance by more than 80% when decreasing external K^+ from 10 mM to submillimolar K^+ concentrations. This K^+ sensitivity of AKT1 reduced K^+ efflux but could not completely prevent K^+ loss. Thus, to overcome adverse potassium loss, plants have evolved a second level of K^+ efflux control. In *Arabidopsis* WT, root cells equip the AKT1 core with the *At*KC1 α-subunit. Heterotetrameric AKT1·*At*KC1 channel complexes operate at even more negative membrane potentials compared with the AKT1 homotetramer (Fig. 4*E*). Consequently, channel activity and thus the potential for K^+ uptake is reduced by incorporating the *At*KC1 subunit into the root channel complex. This apparent negative impact of *At*KC1 on channel performance, however, is more than counterbalanced by its con-

comitant effect on potassium leakage. Based on heteromer formation, the affinity for potassium of the intrinsic K^+ sensor in the channel complex is further decreased (from 16.2 to 26.0 mM). Thus, upon K^+ depletion K^+ loss is thermodynamically strongly disfavored (Fig. 6). Compared with the time scale of many cellular processes, plant root growth represents a conceivable slow process. In this context, reduced K^+ uptake seems rather tolerable compared with K^+ loss. According to our model (Fig. 6), modulation of the gating behavior of the root K^+ inward rectifier by the heteromerization of the two shaker-like α-subunits, AKT1 and *At*KC1, allows fine-tuning of root hair electrophysiological properties in response to the availability of extracellular potassium.

Acknowledgments—We gratefully acknowledge the contributions of Katrin Held, Stephanie Schültke, and Jan Niklas Offenborn in generating some of the CIPK expression constructs used in this study.

REFERENCES

1. Clarkson, D. T., and Hanson, J. B. (1980) *Annu. Rev. Plant Physiol. Plant Mol. Biol.* **31,** 239–298
2. Epstein, E., Rains, D. W., and Elzam, O. E. (1963) *Proc. Natl. Acad. Sci. U.S.A.* **49,** 684–692
3. Lebaudy, A., Véry, A. A., and Sentenac, H. (2007) *FEBS Lett.* **581,** 2357–2366
4. Ward, J. M., Maser, P., and Schroeder, J. I. (2009) *Annu. Rev. Physiol.* **71,** 59–82
5. Fu, H. H., and Luan, S. (1998) *Plant Cell* **10,** 63–73
6. Gierth, M., Mäser, P., and Schroeder, J. I. (2005) *Plant Physiol.* **137,** 1105–1114
7. Kim, E. J., Kwak, J. M., Uozumi, N., and Schroeder, J. I. (1998) *Plant Cell* **10,** 51–62
8. Rubio, F., Santa-Maria, G. E., and Rodriguez-Navarro, A. (2000) *Physiol. Plant.* **109,** 34–43
9. Santa-María, G. E., Danna, C. H., and Czibener, C. (2000) *Plant Physiol.* **123,** 297–306
10. Basset, M., Conejero, G., Lepetit, M., Fourcroy, P., and Sentenac, H. (1995) *Plant Mol. Biol.* **29,** 947–958
11. Dennison, K. L., Robertson, W. R., Lewis, B. D., Hirsch, R. E., Sussman, M. R., and Spalding, E. P. (2001) *Plant Physiol.* **127,** 1012–1019
12. Hirsch, R. E., Lewis, B. D., Spalding, E. P., and Sussman, M. R. (1998) *Science* **280,** 918–921
13. Lagarde, D., Basset, M., Lepetit, M., Conejero, G., Gaymard, F., Astruc, S., and Grignon, C. (1996) *Plant J.* **9,** 195–203
14. Sentenac, H., Bonneaud, N., Minet, M., Lacroute, F., Salmon, J. M., Gaymard, F., and Grignon, C. (1992) *Science* **256,** 663–665
15. Spalding, E. P., Hirsch, R. E., Lewis, D. R., Qi, Z., Sussman, M. R., and Lewis, B. D. (1999) *J. Gen. Physiol.* **113,** 909–918
16. Anderson, J. A., Huprikar, S. S., Kochian, L. V., Lucas, W. J., and Gaber, R. F. (1992) *Proc. Natl. Acad. Sci. U.S.A.* **89,** 3736–3740
17. Brüggemann, L., Dietrich, P., Becker, D., Dreyer, I., Palme, K., and Hedrich, R. (1999) *Proc. Natl. Acad. Sci. U.S.A.* **96,** 3298–3302
18. Ivashikina, N., Becker, D., Ache, P., Meyerhoff, O., Felle, H. H., and Hedrich, R. (2001) *FEBS Lett.* **508,** 463–469
19. Pilot, G., Gaymard, F., Mouline, K., Cherel, I., and Sentenac, H. (2003) *Plant Mol. Biol.* **51,** 773–787
20. Reintanz, B., Szyroki, A., Ivashikina, N., Ache, P., Godde, M., Becker, D., Palme, K., and Hedrich, R. (2002) *Proc. Natl. Acad. Sci. U.S.A.* **99,** 4079–4084
21. Formentin, E., Varotto, S., Costa, A., Downey, P., Bregante, M., Naso, A., Picco, C., Gambale, F., and Lo Schiavo, F. (2004) *FEBS Lett.* **573,** 61–67
22. Duby, G., Hosy, E., Fizames, C., Alcon, C., Costa, A., Sentenac, H., and Thibaud, J. B. (2008) *Plant J.* **53,** 115–123
23. Xu, J., Li, H. D., Chen, L. Q., Wang, Y., Liu, L. L., He, L., and Wu, W. H. (2006) *Cell* **125,** 1347–1360
24. Li, L., Kim, B. G., Cheong, Y. H., Pandey, G. K., and Luan, S. (2006) *Proc. Natl. Acad. Sci. U.S.A.* **103,** 12625–12630
25. Cheong, Y. H., Pandey, G. K., Grant, J. J., Batistic, O., Li, L., Kim, B. G., Lee, S. C., Kudla, J., and Luan, S. (2007) *Plant J.* **52,** 223–239
26. Batistic, O., and Kudla, J. (2009) *Biochim. Biophys. Acta* **1793,** 985–992
27. Lee, S. C., Lan, W. Z., Kim, B. G., Li, L., Cheong, Y. H., Pandey, G. K., Lu, G., Buchanan, B. B., and Luan, S. (2007) *Proc. Natl. Acad. Sci. U.S.A.* **104,** 15959–15964
28. Becker, D., Dreyer, I., Hoth, S., Reid, J. D., Busch, H., Lehnen, M., Palme, K., and Hedrich, R. (1996) *Proc. Natl. Acad. Sci. U.S.A.* **93,** 8123–8128
29. Ishitani, M., Liu, J., Halfter, U., Kim, C. S., Shi, W., and Zhu, J. K. (2000) *Plant Cell* **12,** 1667–1678
30. Walter, M., Chaban, C., Schütze, K., Batistic, O., Weckermann, K., Näke, C., Blazevic, D., Grefen, C., Schumacher, K., Oecking, C., Harter, K., and Kudla, J. (2004) *Plant J.* **40,** 428–438
31. James, P., Halladay, J., and Craig, E. A. (1996) *Genetics* **144,** 1425–1436
32. Naso, A., Montisci, R., Gambale, F., and Picco, C. (2006) *Biophys. J.* **91,** 3673–3683
33. MacKinnon, R. (1991) *Nature* **350,** 232–235
34. Dreyer, I., Antunes, S., Hoshi, T., Müller-Röber, B., Palme, K., Pongs, O., Reintanz, B., and Hedrich, R. (1997) *Biophys. J.* **72,** 2143–2150
35. Daram, P., Urbach, S., Gaymard, F., Sentenac, H., and Chérel, I. (1997) *EMBO J.* **16,** 3455–3463
36. Szyroki, A., Ivashikina, N., Dietrich, P., Roelfsema, M. R., Ache, P., Reintanz, B., Deeken, R., Godde, M., Felle, H., Steinmeyer, R., Palme, K., and Hedrich, R. (2001) *Proc. Natl. Acad. Sci. U.S.A.* **98,** 2917–2921
37. Xicluna, J., Lacombe, B., Dreyer, I., Alcon, C., Jeanguenin, L., Sentenac, H., Thibaud, J. B., and Chérel, I. (2007) *J. Biol. Chem.* **282,** 486–494
38. Pilot, G., Lacombe, B., Gaymard, F., Cherel, I., Boucherez, J., Thibaud, J. B., and Sentenac, H. (2001) *J. Biol. Chem.* **276,** 3215–3221
39. Hertel, B., Horváth, F., Wodala, B., Hurst, A., Moroni, A., and Thiel, G. (2005) *J. Exp. Bot.* **56,** 3103–3110
40. Ortega-Sáenz, P., Pardal, R., Castellano, A., and López-Barneo, J. (2000) *J. Gen. Physiol.* **116,** 181–190
41. Geiger, D., Becker, D., Lacombe, B., and Hedrich, R. (2002) *Plant Cell* **14,** 1859–1868
42. Johansson, I., Wulfetange, K., Porée, F., Michard, E., Gajdanowicz, P., Lacombe, B., Sentenac, H., Thibaud, J. B., Mueller-Roeber, B., Blatt, M. R., and Dreyer, I. (2006) *Plant J.* **46,** 269–281
43. López-Barneo, J., Hoshi, T., Heinemann, S. H., and Aldrich, R. W. (1993) *Receptors Channels* **1,** 61–71
44. Roux, B. T. (2005) *Annu. Rev. Biophys. Biomol. Struct.* **34,** 153–171